Optics and Photonics Journal, 2022, 12, 53-63
https://www.scirp.org/journal/opj
ISSN Online: 2160-889X
ISSN Print: 2160-8881

Scattering by Large Bubbles: Correction for Debye Coefficient at a Small Number of Sub-Waves

Zetian Liu

College of Science, University of Shanghai for Science and Technology, Shanghai, China
Email: dhshevdb@qq.com

How to cite this paper: Liu, Z.T. (2022) Scattering by Large Bubbles: Correction for Debye Coefficient at a Small Number of Sub-Waves. *Optics and Photonics Journal*, **12**, 53-63.
https://doi.org/10.4236/opj.2022.124004

Received: March 21, 2022
Accepted: April 15, 2022
Published: April 18, 2022

Copyright © 2022 by author(s) and Scientific Research Publishing Inc.
This work is licensed under the Creative Commons Attribution International License (CC BY 4.0).
http://creativecommons.org/licenses/by/4.0/
Open Access

Abstract

I found that when the Debye theory calculates the far-field scattered light intensity of bubbles, the forward scattered light intensity is quite different from the result calculated by the Mie theory due to the convergence problem, so the expression of the Debye coefficient has been revised. I derived the Debye reflectance and transmittance according to the physical meaning of Debye theory and compared them with Fresnel's formula. I modified the Debye coefficient expressions for bubbles based on the differences between the Debye reflectance and transmittance from the Fresnel formula. Finally, compared with the far-field scattered light intensity calculated by the original Debye theory, the far-field scattered light intensity calculated based on the modified Debye coefficient can obtain more accurate forward scattered light intensity with fewer sub-waves.

Keywords

Debye Series Expansion, Mie Theory, Bubble, Forward Scattered Light Intensity

1. Introduction

Light scattering of particles is very valuable for the study of metasurfaces [1] and optical tweezers [2]. It has been used widely in various subject areas, such as environmental science, biomedicine, and chemical industry, and applied in environmental monitoring, cell detection, and other technologies [3]. The Lorenz–Mie theory (LMT) proposed a century ago by Mie [4] provides a rigorous way to describe the scattering of a linearly polarized plane wave by a homogeneous sphere. On this basis, Gouesbet [5], Lock [6], Gouesbet, and Gréhan [7] proposed the generalized MLT (GLMT) for the scattering of shaped beams by a spherical particle. However, both LMT and GLMT, which are rigorous electromagnetic theories, give the total effect of scattering, and cannot give the contribution and the physical explanation of various scattering processes. It turns out that writing each term of the Mie infinite series as another infinite series, known as the Debye series, clarifies the physical origins of many effects that occur in electromagnetic scattering [8]-[13].

In ray theory, when a geometrical light ray is an incident upon a dielectric sphere it is partially reflected by the sphere surface, partially transmitted through the sphere, and partially transmitted after making an arbitrary number of internal reflections. Analogously, each term of the Debye-series decomposition of an individual TE or TM partial-wave scattering amplitude may be interpreted as the diffraction of the corresponding spherical multipole wave or its reflection by the sphere surface ($p = 0$) or as transmission through the sphere ($p = 1$) or transmission after making $p-1$ internal reflections ($p \geq 2$). But in the bubble, Debye theory cannot get the correct forward scattered light intensity when the $p_{\max}$ is relatively small like geometric optics. This is because the Debye coefficient converges very slowly when $n > mx$. According to the localization principle, we deduce that the Debye reflectance and transmittance are opposite to the Fresnel formula when the total reflection occurs in geometric optics. Accordingly, we modify the expression of the Debye coefficient to obtain a relatively accurate forward scattered light intensity when $p_{\max}$ is relatively small.

The main structure of this paper is as follows. First, the localization Principle is briefly introduced, which explains the relationship between the order n of the spherical Bessel function and the angle of incidence θ_i in geometric optics. Next, 1) The expressions of Debye reflectance and transmittance are derived and compared with Fresnel's formula. 2) The convergence of Debye coefficients is discussed. 3) Compare the scattered light intensity calculated by Mie theory (this is the exact result) with the Debye scattered light intensity and the geometric scattered light intensity. The expression of Debye scattered light intensity is modified according to the difference between Debye reflectance and transmittance and the Fresnel formula. Finally, this work is summarized.

2. The Localization Principle

Debye's progressive equation proposed in 1908 actually implied the principle of localization principle [14], the localization principle means that in the Mie theory, the light beam containing the n order Bessel function can represent the light incident at the center point $\left(n+\frac{1}{2}\right)\frac{\lambda}{2\pi}$ in the equatorial plane. Debye did not explain the relationship between the Debye series and geometric optics, but after the advent of quantum mechanics, people gave a semi-quantum explanation. The wave equation analogous to the collision of electrons with the perturbation center is the Schrödinger equation, whose solution is in the form of a series with an integer value l (angular momentum quantum number). Electronic de Broglie wavelength is $\lambda = \frac{h}{mv}$ where m is the mass, v is the velocity, h is the Planck constant. If we assume the electron as localized and passing the center at a distance d, the angular momentum $\sqrt{l(l+1)}\frac{h}{2\pi}$ must be equal to mvd. This gives $d = \sqrt{l(l+1)}\frac{\lambda}{2\pi}$. Actually, no exact localization prevails, but the average value of d is $\left(l+\frac{1}{2}\right)\frac{\lambda}{2\pi}$. On this basis, the localization of the Mie terms is not a strict law but a useful guiding principle. On account of the localization principle, we can connect the Debye series of different orders with the geometric rays incident at different positions.

3. Debye Series, Mie Theory and Fresnel Formula

Consider a spherical particle (region 1) with radius a and refractive index m embedded in a vacuum (region 2). The incident wave is a plane wave with wavelength λ. The time dependence is $\exp(-i\omega t)$ with ω being the angular frequency. The geometry of the system is given in Figure 1. When a plane wave is an incident on the particle, the expressions of the incident, internal, and scattered fields can be expanded using vector spherical wave functions (VSWFs) as [15].

$$\begin{aligned}\mathbf{E}_{\text{inc}} &= \sum_{n=1}^{\infty} E_n\left(\mathbf{M}_{o1n}^{(1)} - i\mathbf{N}_{e1n}^{(1)}\right)\\ \mathbf{H}_{\text{inc}} &= -\frac{k_1}{\omega\mu_1}\sum_{n=1}^{\infty} E_n\left(\mathbf{M}_{e1n}^{(1)} + i\mathbf{N}_{o1n}^{(1)}\right)\end{aligned} \tag{1}$$

$$\begin{aligned}\mathbf{E}_{\text{int}} &= \sum_{n=1}^{\infty} E_n\left(c_n\mathbf{M}_{o1n}^{(1)} - id_n\mathbf{N}_{e1n}^{(1)}\right)\\ \mathbf{H}_{\text{int}} &= -\frac{k_1}{\omega\mu_1}\sum_{n=1}^{\infty} E_n\left(d_n\mathbf{M}_{e1n}^{(1)} + ic_n\mathbf{N}_{o1n}^{(1)}\right)\end{aligned} \tag{2}$$

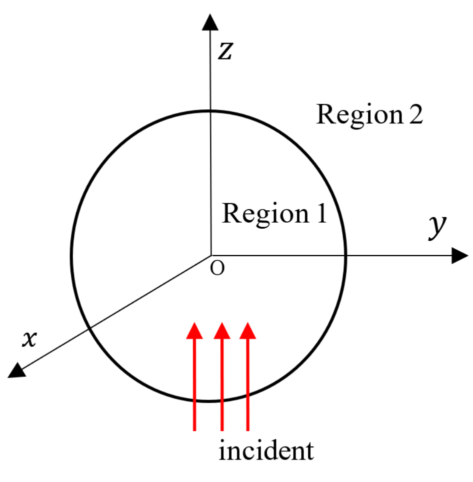

Figure 1. Geometry for a charged sphere illuminated by a plane wave.

$$\begin{aligned}\mathbf{E}_{\text{sca}} &= \sum_{n=1}^{\infty} E_n \left(i a_n \mathbf{N}_{e1n}^{(3)} - b_n \mathbf{M}_{o1n}^{(3)} \right) \\ \mathbf{H}_{\text{sca}} &= \frac{k_2}{\omega \mu_2} \sum_{n=1}^{\infty} E_n \left(a_n \mathbf{M}_{e1n}^{(3)} + i b_n \mathbf{N}_{o1n}^{(3)} \right)\end{aligned} \tag{3}$$

where subscripts inc, int, and sca represent the incident, internal, and scattered fields, respectively. $E_n = E_0 \cdot i^n (2n+1)/n/(n+1)$ with E_0 is the amplitude of the incident plane wave. $k_1 = m_1 2\pi/\lambda$ and $k_2 = m_2 2\pi/\lambda$ are the wavenumbers in the sphere and in the surrounding media, respectively. μ_1 and μ_2 are the permeabilities of the sphere and surrounding media, respectively. In this paper, we assume that the sphere is non-magnetic ($\mu_1 = \mu_2 = \mu_0$ with μ_0 being the permeabilities in a vacuum). $x = k_2 a$ and $y = k_1 a = \frac{m_1}{m_2} x = mx$, m is the relative refractive index. $\mathbf{M}_{o1n}^{(j)}$, $\mathbf{M}_{e1n}^{(j)}$, $\mathbf{N}_{o1n}^{(j)}$ and $\mathbf{N}_{e1n}^{(j)}$ are VSWFs 15. (a_n, b_n, c_n, d_n) are the Mie scattering coefficients [16]. Mie scattering amplitude is [17]:

$$\begin{aligned}S_{M1}(x,m,\theta) &= \sum_{n=1}^{\infty} \frac{2n+1}{n(n+1)} \left[a_n(x,m)\pi_n(\cos\theta) + b_n(x,m)\tau_n(\cos\theta) \right] \\ S_{M2}(x,m,\theta) &= \sum_{n=1}^{\infty} \frac{2n+1}{n(n+1)} \left[a_n(x,m)\tau_n(\cos\theta) + b_n(x,\mathrm{m})\pi_n(\cos\theta) \right]\end{aligned} \tag{4}$$

where, the scattering angle function is obtained by $\pi_n = P_n^1(\cos\theta)/\sin\theta$, $\tau_n = \mathrm{d}P_n^1(\cos\theta)/\mathrm{d}\theta$, P_n^1 is the associated Legendre function of the nth order and the 1st degree.

The average Mie scattered light intensity is

$$i_M(x,m,\theta) = \frac{\left|S_{M1}(x,m,\theta)\right|^2 + \left|S_{M2}(x,m,\theta)\right|^2}{2} \tag{5}$$

When the time-harmonic factor $\mathrm{e}^{-i\omega t}$ is used, the radial function of the outward wave has the form of the spherical Hank function of the first kind ($h_n^{(1)}(m_2 kr)$), and the radial function of the inward wave has the form of the spherical Hank function of the second kind ($h_n^{(2)}(m_2 kr)$). Therefore, the incident wave can be written in the form of $A\frac{h_n^{(2)}(m_2 kr)}{h_n^{(2)}(x)}$ (where the coefficients A will be considered later), the reflected wave is written in $A \cdot r_n^{212} \frac{h_n^{(1)}(m_2 kr)}{h_n^{(1)}(x)}$, and the transmitted wave is shown as $A \cdot t_n^{21} \frac{h_n^{(2)}(m_1 kr)}{h_n^{(2)}(y)}$. The values of the incident wave, reflected wave and transmitted wave at the spherical surface are A, $A \cdot r_n^{212}$ and $A \cdot t_n^{21}$ respectively. Therefore, r_n^{212} and t_n^{21} represent the reflection coefficient and transmission coefficient of the light wave propagating from the outside to the inside of the ball, singly. In this case, the waves in regions 1 and 2 are written as (omitting the angular function):

$$\begin{aligned}\psi_1 &= A\cdot t_n^{21}\frac{h_n^{(2)}(m_1kr)}{h_n^{(2)}(y)} && \text{for } r\le a\\ \psi_2 &= A\left[\frac{h_n^{(2)}(m_2kr)}{h_n^{(2)}(x)}+r_n^{212}\frac{h_n^{(1)}(m_2kr)}{h_n^{(1)}(x)}\right] && \text{for } r\ge a\end{aligned}\tag{6}$$

The reflection and transmission of light waves when propagating from the inside of the sphere to outside the sphere can be given in the same way as Equation (6):

$$\begin{aligned}\psi_1 &= A\left[\frac{h_n^{(1)}(m_1kr)}{h_n^{(1)}(y)}+r_n^{121}\frac{h_n^{(2)}(m_1kr)}{h_n^{(2)}(y)}\right] && \text{for } r\le a\\ \psi_2 &= A\cdot t_n^{12}\frac{h_n^{(1)}(m_2kr)}{h_n^{(1)}(x)} && \text{for } r\ge a\end{aligned}\tag{7}$$

Among them, r_n^{121} and t_n^{12} respectively represent the reflection coefficient and transmission coefficient when the light wave propagates from the inside to the outside of the sphere. Below we solve the reflection coefficient and transmission coefficient r_n^{212}, r_n^{121}, t_n^{21} and t_n^{12} in the case of TE wave and TM wave.

According to the electromagnetic wave theory, the boundary condition of the electromagnetic field is that the transverse components of the electric field and the magnetic field are continuous. For TE waves (see Equations (1), (2), and (3)), the continuity of the electric field quantity is reflected in the radial function $z_n(\rho)$ being equal on both sides of the interface, and the continuity of the magnetic field quantity is equal on both sides of the interface by $k\left[\rho z_n(\rho)\right]'/\mu/\rho$. For the TM wave, it can be obtained from seeing Equations (1), (2), and (3) that the continuity of the electric field is equal to $\left[\rho z_n(\rho)\right]'/\rho$ on both sides of the interface, and the continuity of the magnetic field is equal to $kz_n(\rho)/\mu$ on both sides of the interface.

Hence, for TE waves, Equations (6) and (7) can be obtained as:

$$\begin{aligned}&t_n^{21}=1+r_n^{212}\\ &\frac{k_1}{\mu_1}t_n^{21}\frac{\left[yh_n^{(2)}(y)\right]'}{yh_n^{(2)}(y)}=\frac{k_2}{\mu_2}\left\{\frac{\left[xh_n^{(2)}(x)\right]'}{xh_n^{(2)}(x)}+r_n^{212}\frac{\left[xh_n^{(1)}(x)\right]'}{xh_n^{(1)}(x)}\right\}\\ &1+r_n^{121}=t_n^{12}\\ &\frac{k_1}{\mu_1}\left\{\frac{\left[yh_n^{(1)}(y)\right]'}{yh_n^{(1)}(y)}+r_n^{121}\frac{\left[yh_n^{(2)}(y)\right]'}{yh_n^{(2)}(y)}\right\}=\frac{k_2}{\mu_2}t_n^{12}\frac{\left[xh_n^{(1)}(x)\right]'}{xh_n^{(1)}(x)}\end{aligned}\tag{8}$$

Similarly, the TM waves can be obtained by Equations (6) and (7):

$$\frac{k_1}{\mu_1}t_n^{21}=\frac{k_2}{\mu_2}\left(1+r_n^{212}\right)$$

$$t_n^{21}\frac{\left[yh_n^{(2)}(y)\right]'}{yh_n^{(2)}(y)}=\frac{\left[xh_n^{(2)}(x)\right]'}{xh_n^{(2)}(x)}+r_n^{212}\frac{\left[xh_n^{(1)}(x)\right]'}{xh_n^{(1)}(x)}$$

$$\begin{gathered}\frac{k_1}{\mu_1}\left(1+r_n^{121}\right)=\frac{k_2}{\mu_2}t_n^{12}\\ \frac{\left[yh_n^{(1)}(y)\right]'}{yh_n^{(1)}(y)}+r_n^{121}\frac{\left[yh_n^{(2)}(y)\right]'}{yh_n^{(2)}(y)}=t_n^{12}\frac{\left[xh_n^{(1)}(x)\right]'}{xh_n^{(1)}(x)}\end{gathered} \tag{9}$$

Solving Equations (8) and (9) comparing their solutions, we can find that they have the same form.

$$\begin{aligned}r_n^{212}&=-\frac{\alpha D_n^{(4)}(x)-\beta D_n^{(4)}(y)}{\alpha D_n^{(3)}(x)-\beta D_n^{(4)}(y)}\\ t_n^{21}&=\mu\frac{D_n^{(3)}(x)-D_n^{(4)}(x)}{\alpha D_n^{(3)}(x)-\beta D_n^{(4)}(y)}\\ r_n^{121}&=-\frac{\alpha D_n^{(3)}(x)-\beta D_n^{(3)}(y)}{\alpha D_n^{(3)}(x)-\beta D_n^{(4)}(y)}\\ t_n^{12}&=m\frac{D_n^{(3)}(y)-D_n^{(4)}(y)}{\alpha D_n^{(3)}(x)-\beta D_n^{(4)}(y)}\end{aligned} \tag{10}$$

Here we will define some parameters:

$D_n^{(j)}(x)=\dfrac{Z_n^{(j)\prime}(z)}{Z_n^{(j)}(z)}$, $\alpha=\begin{cases}\mu & \text{TE wave}\\ m & \text{TM wave}\end{cases}$ and $\beta=\begin{cases}m & \text{TE wave}\\ \mu & \text{TM wave}\end{cases}$; where $Z_n^{(j)}(\rho)$ is the Riccati-Bessel function of the *j*-th kind.

The Fresnel equationis:

$$\begin{aligned}r_\perp&=\frac{\cos\theta_i-m\cos\theta_t}{\cos\theta_i+m\cos\theta_t}\\ t_\perp&=\frac{2\cos\theta_i}{\cos\theta_i+m\cos\theta_t}\\ r_\parallel&=\frac{m\cos\theta_i-\cos\theta_t}{m\cos\theta_i+\cos\theta_t}\\ t_\parallel&=\frac{2\cos\theta_i}{m\cos\theta_i+\cos\theta_t}\end{aligned} \tag{11}$$

θ_t can be known from the Snell equation:

$$\sin\theta_i=m\sin\theta_t \tag{12}$$

According to the localization principle (The spherical Bessel function is a half-integer order Bessel function):

$$\sin\theta_i=\frac{l+0.5}{k_2a}=\frac{n}{x} \tag{13}$$

By comparing Equations (10) and (11) we can gain the relation between the Debye equation and the Fresnel equation.

The incidence angle of the Fresnel formula in **Figure 2** is related to the particle size a and the order n. That is, it is calculated by Equation (13). When $n = mx$, the incident angle is exactly the critical angle of total reflection. So from $n = mx$ to $n = x$, the imaginary parts of Debye reflectance and transmittance are

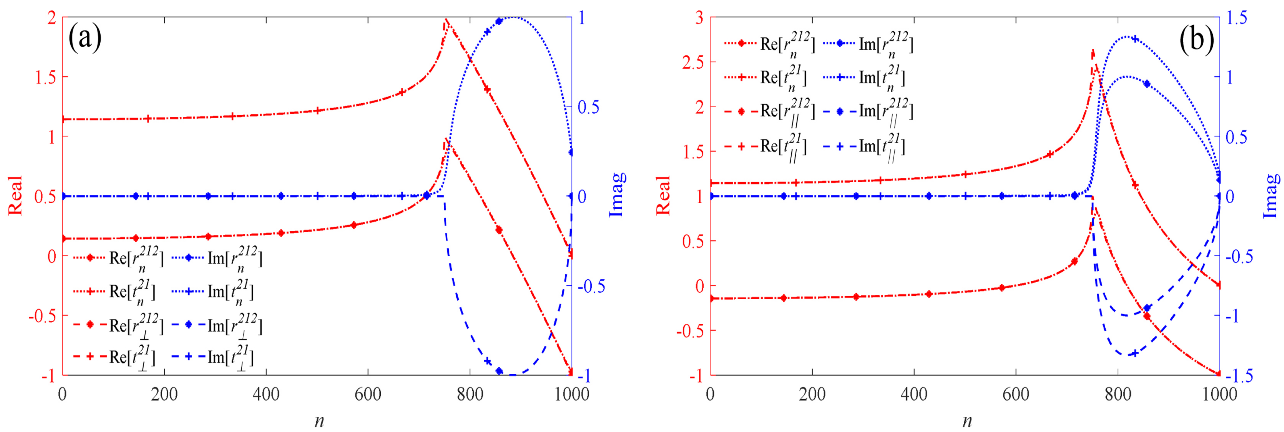

Figure 2. When a plane wave irradiates a spherical bubble with dimensionless particle size $x = 1000$ and a relative refractive index $m = 0.75$, the reflectance and transmittance vary with n: (a) The incident wave is TE wave; (b) the incident wave in figure b is TM wave.

exactly the opposite of those calculated by the Fresnel formula. We found this phenomenon, but couldn't explain it very well. And it will affect the accuracy of Debye's scattered light intensity.

From the literature [18] we can know the relationship between the Debye scattering coefficient and the Mie scattering coefficient:

$$\begin{matrix} A_n^{(0,p_{\max})} \\ B_n^{(0,p_{\max})} \end{matrix} + \frac{1}{2} = \frac{1}{2} - \frac{1}{2}\frac{h_n^{(2)}(x)}{h_n^{(1)}(x)}\left\{ r_n^{212} + t_n^{21}\frac{h_n^{(1)}(y)}{h_n^{(2)}(y)} t_n^{12} \frac{1-\left[\frac{h_n^{(1)}(y)}{h_n^{(2)}(y)} r_n^{121}\right]^{p_{\max}}}{1-\frac{h_n^{(1)}(y)}{h_n^{(2)}(y)} r_n^{121}} \right\} \approx \begin{matrix} a_n \\ b_n \end{matrix} \tag{14}$$

Here, $(0, p_{\max})$ represents the summation of terms from 0 to $p_{\max}$, and $p_{\max}$ represents the calculation up to the $p_{\max}$ -thsubwave. At the same time, the r_n^{212}, t_n^{21}, r_n^{121}, and t_n^{12} of the TE wave need to be used when solving $B_n^{(0,p_{\max})}$; When solving $A_n^{(0,p_{\max})}$, we need to use the parameters of the TM wave.

The results in **Figure 3** show that when $n > 750$, the convergence of the Debye coefficients becomes worse and worse. When $n = 1000$, $p_{\max}$ needs to be greater than 10^{230} 10 Debye coefficient to converge to the Mie coefficient.

Like Mie scattering, Debye scattering amplitude is

$$\begin{aligned} S_{D1}(x,m,\theta) &= \sum_{n=1}^{\infty}\sum_{p_{\max}}^{\infty}\frac{2n+1}{n(n+1)}\left[\left(A_n^{(0,p_{\max})}(x,m)+\frac{1}{2}\right)\pi_n(\cos\theta)\right. \\ &\quad \left.+\left(B_n^{(0,p_{\max})}(x,m)+\frac{1}{2}\right)\tau_n(\cos\theta)\right] \\ S_{D2}(x,m,\theta) &= \sum_{n=1}^{\infty}\sum_{p_{\max}}^{\infty}\frac{2n+1}{n(n+1)}\left[\left(A_n^{(0,p_{\max})}(x,m)+\frac{1}{2}\right)\tau_n(\cos\theta)\right. \\ &\quad \left.+\left(B_n^{(0,p_{\max})}(x,m)+\frac{1}{2}\right)\pi_n(\cos\theta)\right] \end{aligned} \tag{15}$$

The average Debye scattered light intensity is

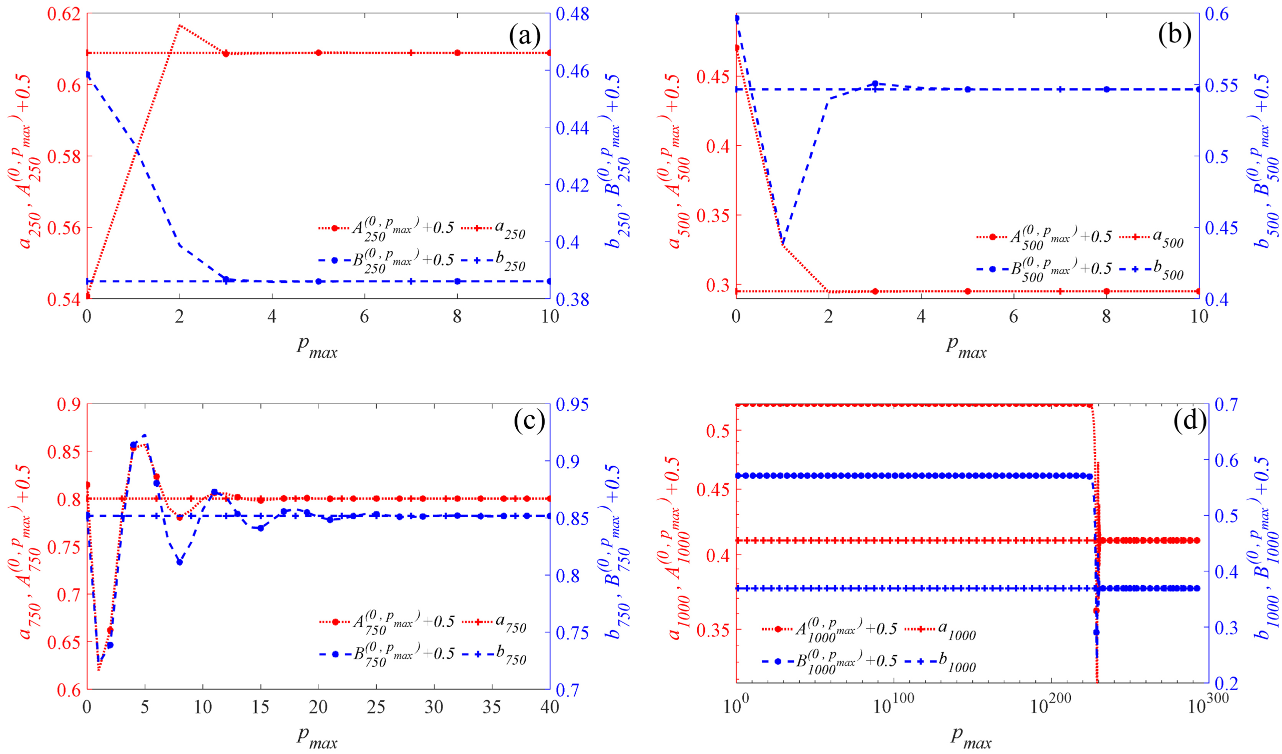

Figure 3. When a plane wave irradiates a spherical bubble with dimensionless particle size $x = 1000$ and a relative refractive index $m = 0.75$, Convergence of $A_n^{(0,p_{\max})} + 0.5$ and $B_n^{(0,p_{\max})} + 0.5$ with $p_{\max}$: (a) $n = 250$; (b) $n = 500$; (c) $n = 750$; (d) $n = 1000$.

$$i_D(x,m,\theta) = \frac{\left|S_{D1}(x,m,\theta)\right|^2 + \left|S_{D2}(x,m,\theta)\right|^2}{2} \tag{16}$$

The following is mainly to compare the difference in far-field scattered light intensity of Debye theory, geometric optics approximation, and Mie theory. And for bubbles, the scattered light intensity of Debye theory is corrected.

The purpose of this paper is to make corrections for the Debye scattered light intensity of bubbles in the case of fewer sub-waves ($p_{\max}$). The geometrical optics approximation is mentioned here mainly because it is based on the Fresnel formula. The basis for the correction of the Debye scattered light intensity in this paper is that the Debye reflectance and transmittance are inconsistent with the Fresnel formula. The geometrical optics approximation will not give exactly the same results as Mie theory which turns out to be accurate since it does not take into account surface waves, etc. [19], and it is the most time-consuming algorithm here.

In the legend of **Figure 4**, GOA-Yu refers to the far-field scattered light intensity calculated by Yu *et al.* [19]. based on geometric optics approximation; Mie refers to the far-field scattered light intensity calculated using Mie theory (Equation (5)); Debey refers to the far-field scattered light intensity calculated using Debey theory (Equations (14), (15), and (16)); Observing **Figure 4(a)**, the geometric optics approximation is basically consistent with the Mie theory except for the scattered light intensity near 80 degrees, which Yu *et al.* discussed in their

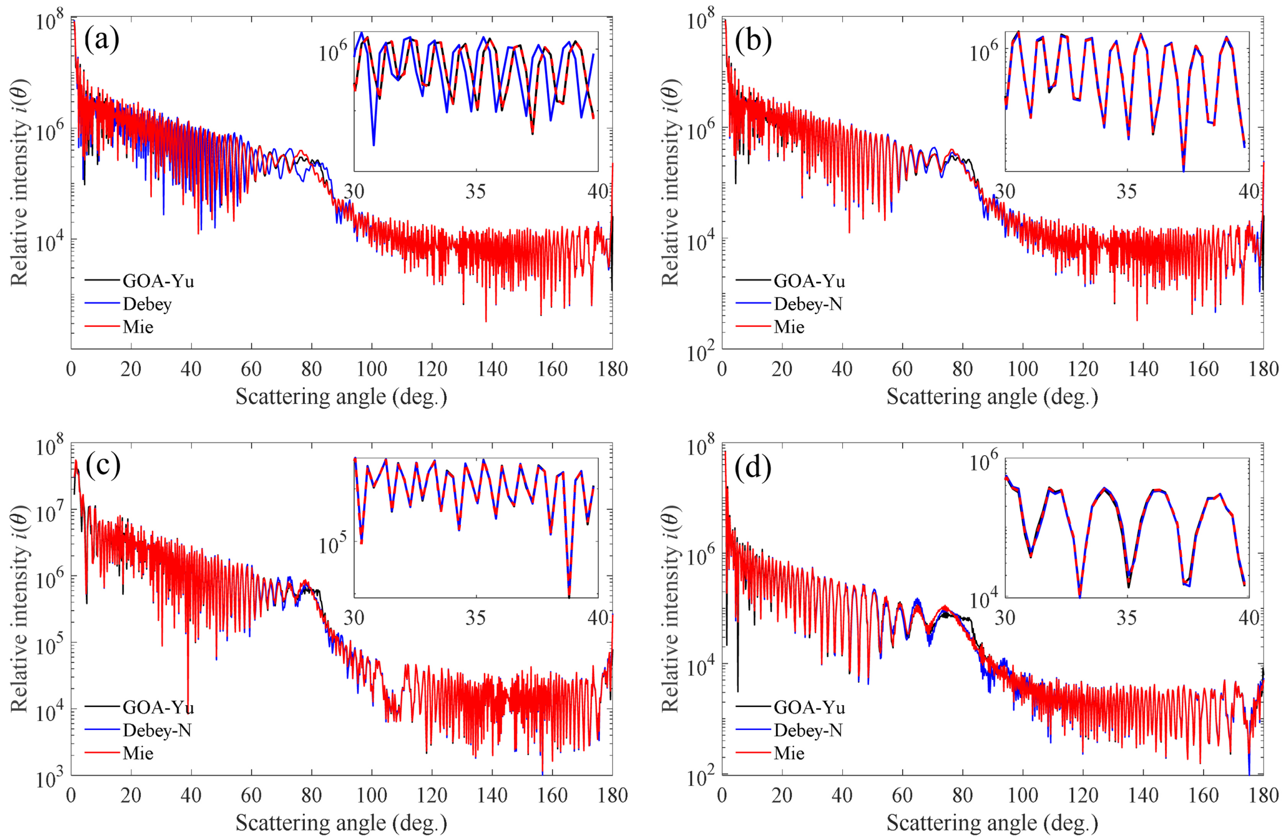

Figure 4. When a plane wave irradiates a spherical bubble with a relative refractive index $m = 0.75$, $p_{\max} = 10$, far-field scattered light intensity calculated by different algorithms: (a) $x = 1000$, Original Debye scattered light intensity; (b) $x = 1000$; (c) $x = 1500$; (d) $x = 2000$.

paper 19. When the refractive index of the particle $m < 1$, the difference between the Debye theory and the forward scattered light intensity of the two is more obvious, but this phenomenon does not appear in the particle with $m > 1$. This is easy to understand. As mentioned earlier, when $n > mx$, the Debye coefficient convergence will get worse and worse. It will not converge when $p_{\max} = 10$. Considering that the Debye reflectance and transmittance are conjugated to the Fresnel results when $n > mx$, we modified Equation (14) to obtain Equation (17). where * stands for complex conjugate.

$$\frac{A_n^{(0,p_{\max})\prime}}{B_n^{(0,p_{\max})\prime}} + \frac{1}{2} = \frac{1}{2} - \frac{1}{2}\frac{h_n^{(2)}(x)}{h_n^{(1)}(x)} \begin{cases} r_n^{212} + t_n^{21}\dfrac{h_n^{(1)}(y)}{h_n^{(2)}(y)} t_n^{12} \dfrac{1 - \left[\dfrac{h_n^{(1)}(y)}{h_n^{(2)}(y)} r_n^{121}\right]^{p_{\max}}}{1 - \dfrac{h_n^{(1)}(y)}{h_n^{(2)}(y)} r_n^{121}} & n \le mx \\ r_n^{212*} + t_n^{21*}\dfrac{h_n^{(1)}(y)}{h_n^{(2)}(y)} t_n^{12*} \dfrac{1 - \left[\dfrac{h_n^{(1)}(y)}{h_n^{(2)}(y)} r_n^{121}\right]^{p_{\max}}}{1 - \dfrac{h_n^{(1)}(y)}{h_n^{(2)}(y)} r_n^{121}} & n > mx \end{cases} \tag{17}$$

Debey-N in the legends of Figures 4(b)-(d) is our improved Debye algorithm. This algorithm is calculated by Equations (14), (15) and (16).

The calculation results for bubbles show that when $p_{\max}$ is relatively small, our improved Debye scattering light intensity algorithm is close to the Mie algorithm. This is a significant improvement in the accuracy of the original Debye algorithm.

4. Conclusion

In this work, we describe the problem that the imaginary part of Debye reflectance and transmittance is opposite to the Fresnel equation when the relative refractive index is less than 1 and total reflection occurs in geometric optics. Secondly, we explained the conditions for the slow convergence of the Debye partial wave coefficients. And we give the partial wave convergence graph. Finally, we improved the calculation of Debye scattered light intensity, so that it can obtain a more accurate scattered light intensity even when $p_{\max}$ is relatively small. It is worth noting that this improvement is only based on part of the physical meaning of Debye's theory, but the effect is obvious. If you want to get the accurate scattered light intensity through Debye theory, you need to calculate it through the original formula, and $p_{\max}$ needs to be large enough, which is undoubtedly very time-consuming and very easy to overflow.

Conflicts of Interest

The author declares no conflicts of interest regarding the publication of this paper.

References

[1] Proust, J., Bedu, F., Gallas, B., Ozerov, I. and Bonod, N. (2016) All-Dielectric Colored Metasurfaces with Silicon Mie Resonators. *ACS Nano*, **10**, 7761-7767. https://doi.org/10.1021/acsnano.6b03207

[2] Curtis, J.E., Koss, B.A. and Grier, D.G. (2002) Dynamic Holographic Optical Tweezers. *Optics Communications*, **207**, 169-175. https://doi.org/10.1016/S0030-4018(02)01524-9

[3] Van de Hulst, H.C. (1981) Light Scattering by Small Particles. Courier Corporation, Chelmsford, MA.

[4] Mie, G. (1908) Beiträge zur Optik trüber Medien, speziell kolloidaler Metallösungen. *Annalen der Physik*, **330**, 377-445. https://doi.org/10.1002/andp.19083300302

[5] Gouesbet, G., Maheu, B. and Gréhan, G. (1988) Light Scattering from a Sphere Arbitrarily Located in a Gaussian Beam, Using a Bromwich Formulation. *Journal of the Optical Society of America A*, **5**, 1427-1443. https://doi.org/10.1364/JOSAA.5.001427

[6] Lock, J.A. (1993) Contribution of High-Order Rainbows to the Scattering of a Gaussian Laser Beam by a Spherical Particle. *Journal of the Optical Society of America A*, **10**, 693-706. https://doi.org/10.1364/JOSAA.10.000693

[7] Gouesbet, G. and Gréhan, G. (2011) Generalized Lorenz-Mie Theories. Springer, Berlin. https://doi.org/10.1007/978-3-642-17194-9

[8] Van der Pol, B. and Bremmer, H. (1937) XIII. The Diffraction of Electromagnetic Waves from an Electrical Point Source Round a Finitely Conducting Sphere, with Applications to Badiotelegraphy and the Theory of the Rainbow—Part I. *The London, Edinburgh, and Dublin Philosophical Magazine and Journal of Science*, **24**, 141-176. https://doi.org/10.1080/14786443708561897

[9] Nussenzveig, H.M. (1969) High-Frequency Scattering by a Transparent Sphere. I. Direct Reflection and Transmission. *Journal of Mathematical Physics*, **10**, 82-124. https://doi.org/10.1063/1.1664764

[10] Nussenzveig, H.M. (1969) High-Frequency Scattering by a Transparent Sphere. II. Theory of the Rainbow and the Glory. *Journal of Mathematical Physics*, **10**, 125-176. https://doi.org/10.1063/1.1664747

[11] Khare, V. (1976) Short-Wavelength Scattering of Electromagnetic Waves by a Homogeneous Dielectric Sphere. Ph.D. Thesis, University of Rochester, New York.

[12] Lock, J.A. (1988) Cooperative Effects among Partial Waves in Mie Scattering. *Journal of the Optical Society of America A*, **5**, 2032-2044. https://doi.org/10.1364/JOSAA.5.002032

[13] Lock, J.A. and Hovenac, E.A. (1991) Internal Caustic Structure of Illuminated Liquid Droplets. *Journal of the Optical Society of America A*, **8**, 1541-1552. https://doi.org/10.1364/JOSAA.8.001541

[14] Debye, P. (1908) Das elektromagnetische Feldum einen Zylinder und die Theorie des Regenbogens. *Physikalische Zeitschrift*, **9**, 775-778.

[15] Bohren, C.F. and Huffman, D.R. (2008) Absorption and Scattering of Light by Small Particles. John Wiley & Sons, Hoboken, NJ.

[16] Gouesbet, G. (2020) Van de Hulst Essay: A Review on Generalized Lorenz-Mie theories with Wow Stories and an Epistemological Discussion. *Journal of Quantitative Spectroscopy and Radiative Transfer*, **253**, Article ID: 107117. https://doi.org/10.1016/j.jqsrt.2020.107117

[17] Van de Hulst, H.C. (1957) Light Scattering by Small Particles. John Wiley and Sons, New York; Chapman and Hall, London. https://doi.org/10.1063/1.3060205

[18] Shen, J. and Wang, H. (2010) Calculation of Debye Series Expansion of Light Scattering. *Applied Optics*, **49**, 2422-2428. https://doi.org/10.1364/AO.49.002422

[19] Yu, H., Shen, J. and Wei, Y. (2008) Geometrical Optics Approximation of Light Scattering by Large Air Bubbles. *Particuology*, **6**, 340-346. https://doi.org/10.1016/j.partic.2008.07.003